Tomographic Imaging of Cracked Pier Cap of Evans over Santa Fe Bridge

By Kevin L. Rens and David J. Transue

A tomographic study of a pier cap of the Evans over Santa Fe Bridge, located in Denver, Colorado, was performed. The pier cap shows cracks on vertical and horizontal surfaces, as shown in Figures 1 and 2. The purpose of this study was to evaluate the interior condition of the beam. In particular, it was desired to determine the depth of penetration of the cracks observed on the surface.

Equipment

Piezo-electric ultrasonic transducers were used to generate stress waves in the concrete and to receive the resulting waveforms. A 1.5-in.-diameter transducer was used as the sending transducer while a 1/8-in.-diameter transducer was the receiving transducer. A computer equipped with a 1000 V-pulse generator and a 10 MHz-data acquisition card was used to excite the sending transducer and to record the waveform from the receiving transducer. The received waveforms were amplified with an ultrasonic preamplifier. The travel times for this equipment are accurate to better than 1 micro-second for sampling rates greater than 1 MHz. (Further information on the software, hardware, and theory can be found in the Appendix).

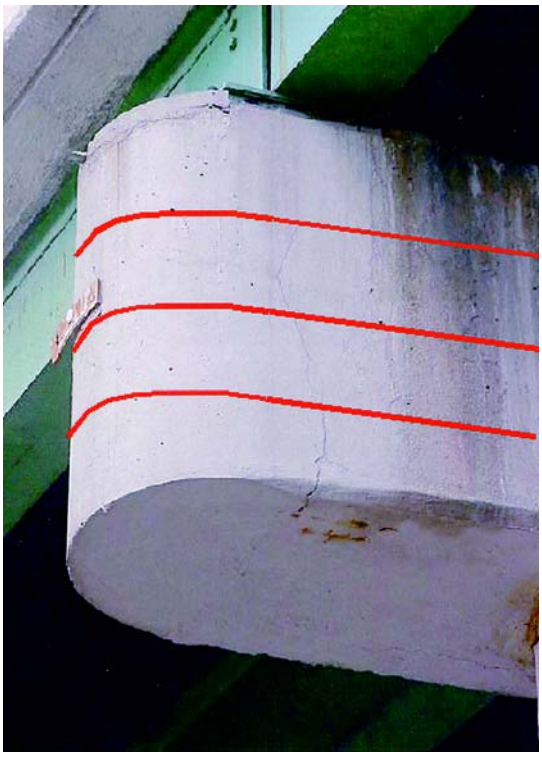

Figure 1: The surface of the pier cap from the east, showing cracks. The perimeters of the three imaging planes are shown in red

Data Collection Procedure

The pier cap was accessed using two man-lifts, one positioned on each side of the beam. Waveform data were taken from points on the perimeter of three horizontal cross sections of the blocks. Once the grid of points along the perimeter was established, the sending transducer was affixed to one of the points, and wave pulses were sent into the concrete. The receiving transducer was then used to receive stress waves at the remaining points on

Figure 2: Detail of the pier cap from the west, showing cracks

Table 1: Location of imaging plane; number of measurements; and average, maximum, and minimum velocities recorded in each data set

Location of Imaging Plane	# Rays	Average Pulse Velocity (meters/second)	Maximum Pulse Velocity (meters/second)	Minimum Pulse Velocity (meters/second)
11 inches	106	3362	4303	1792
23 inches	101	3195	4414	1821
35 inches	109	3601	4074	2606

the perimeter where the waveform was discernable. The sending transducer was then moved to the next point on the perimeter, and the procedure was repeated. Each transmission from the sending to the receiving transducer, or ray, was described by the coordinates of its sending and receiving locations and the time of travel of the wave transmission. Figure 3 shows all of the rays, or the ray-path mesh, of the imaged cross sections.

Data and Observations

Three horizontal cross sections were imaged. Table 1 shows the number of rays used for each image and the average, maximum, and minimum velocities recorded for each data set. These results provide an indication of the relative quality of concrete in each cross section.

Figure 4 shows ray-path velocities for all rays that propagated directly across the pier cap in the E-W direction. These ray velocities provide a useful comparison to, and a check of, the tomograms.

Several tomographic analyses were performed using straight-ray and curved-ray analysis techniques. The result of the analysis is a map of the velocity field in each cross section (tomogram). The tomograms are shown in Figure 5.

Analysis

The crack drawn in the lower left quadrant of the images appears to propagate into the pier a distance of 40 to 50% of the width of the pier cap in the lower portion of the pier, as seen in the images from 11 and 23 in. above the bottom of the pier. The crack appears as a low velocity region, and is "smeared" over an area. The image at 35 in. shows that the crack propagates approximately 8 in. into the pier, indicating that the crack becomes smaller at the top of the pier cap.

The crack drawn in the upper left quadrant of the images appears to propagate into the pier a distance of 25 to 35% of the width of the pier cap in the image at 11 in. from the bottom of the pier. This crack appears to propagate approximately 8 in. into the pier at 23 in. above the bottom. The crack does not propagate upwards into the plane imaged at 35 in. above the bottom of the pier. Given

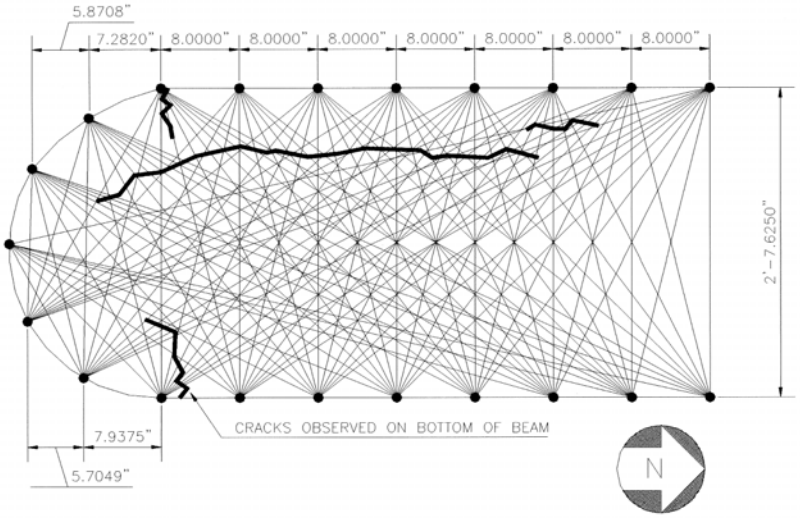

Figure 3: Ray-path mesh of the beam section. One ultrasonic pulse velocity measurement was made along each ray path shown. Three sections were imaged using this pattern of measurements: one at 11 in., one at 23 in., and one at 35 in. above the bottom of the beam. Cracks observed from the bottom of the beam are shown

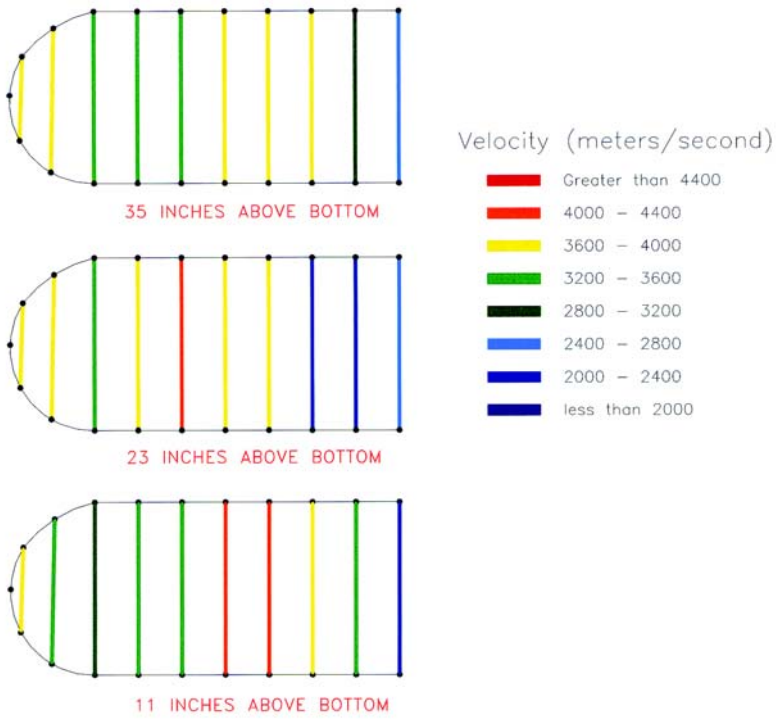

Figure 4: Straight-ray velocity measurements in the E-W direction for the three imaging planes

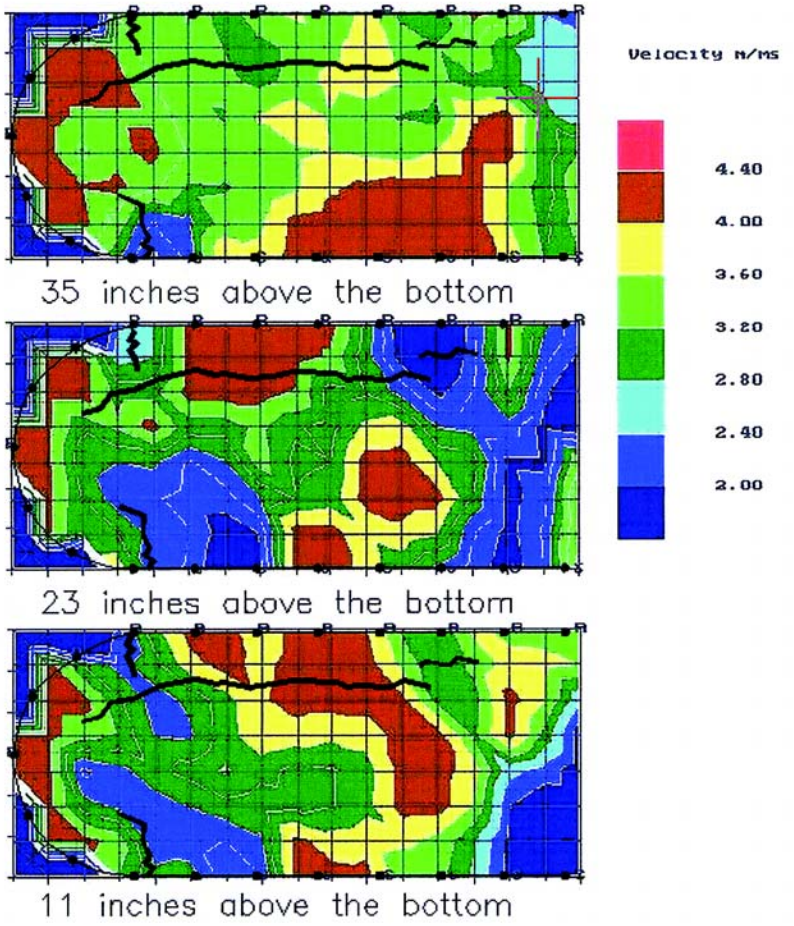

Figure 5: Tomograms of the three imaging planes. These images were formed using 10 iterations of the simultaneous iterative reconstruction technique (SIRT) algorithm (see Appendix). The observed cracks, depicted in black, were superimposed over the image. These cracks were observed on the bottom surface of the pier cap. The outline of the pier cap and the sending and receiving coordinates were also overlayed. The corners on the left ends of the images were out of the boundaries of the pier cap, and are not a part of the analyses

that in all cases there is a higher velocity region separating the two cracks, it does not appear that the two cracks are continuous.

The crack running longitudinally, drawn on the top side of the images, does not seem to affect the velocity field.

The very high velocities shown at the "bull-nose" of the pier cap are accentuated by the imaging algorithm. This region can be assumed to be sound concrete.

The low velocity region on the right side of the lower two images is likely due to poorly consolidated concrete in the reinforcing cage of the pier, which intersects the image plane at that location. The high velocity region just to the left of these regions may be due to the velocity-increasing effect of the hoop reinforcing steel, and to the presence of a region of relatively well-consolidated and uncracked concrete.

Ultrasonic tomography is a well-developed imaging technique for large-grained building materials such as concrete, masonry, and rock. It was successfully applied to the pier cap in this example, and the analysis determined that the visible cracks do not compromise safety. Advanced inspection technology is not necessarily an integral everyday assessment device. However, when used as a tool to further visual inspections, a better condition assessment can be made. Sometimes, nondestructive evaluation technology can prevent failures; other times, as in the case of this bridge pier cap, unnecessary major rehabilitation can be avoided. Tomography can be further used in determining the effectiveness of any repair that may occur. For example, it is recommended that although the existing cracks do not compromise

APPENDIX

Overview of Tomographic Method

The following sections describe the basic theory of ultrasonic tomography. For more detail on the hardware, software, and theory utilized in this study, refer to Transue et al.[1] and Rens et al.[2]

Straight Ray-Path Tomography

Tomography is the practice of constructing a cross-sectional image of an object from transmissions (or reflections) of waves or radiation through the object. A property of the transmission, such as the travel time of a stress wave or the attenuation of an electromagnetic wave, is measured. These measurements are typically made from one point to another along the perimeter of the object. Figure 3 in the main body of this document shows typical meshes of intersecting ray paths through a cross section. The nodes on the perimeter of the mesh indicate the transmission and reception points of each ray. It is desired to solve for the velocity field $v(x,y)$ or the relative attenuation field, alpha (x,y), of a cross section within the perimeter of the measurements. A line integral is used to express the measured parameter as a function of the velocity (or attenuation) field along the ray path. Techniques for solving this problem include direct matrix inversion, Fourier transform methods, convolutional or back-projection methods, and iterative techniques such as the algebraic reconstruction technique (ART) and the simultaneous iterative reconstruction technique (SIRT). All of the cases in this study use the SIRT algorithm to solve for the slowness (inverse velocity) field, and the remainder of this discussion is limited to this situation.

A continuous function $v(x,y)$ cannot be solved for

safety, they should indeed be sealed. One sealing method might include epoxy injection. Epoxy-filled cracks will show up as faster velocity regions when compared with air voids, cracks, or solid concrete. By completing a tomogram after repairs, it can be determined if the crack voids are completely filled.

References

1. Transue, D. J.; Rens, K. L.; and Schuller, M. P., "A Study of the Practicality of Acoustic Tomographic Imaging for the NDE of Concrete Structures," *Infrastructure Condition Assessment: Art, Science, and Practice*, Mitsuru Saito, ed., American Society of Civil Engineers, New York, 1997.

2. Rens, K. L.; Transue, D. J.; and Schuller M. P., "Acoustic Tomographic Imaging of Concrete Infrastructure," *Journal of Infrastructure Systems*, American Society of Civil Engineers, New York, V. 6, No. 1, 2000, pp. 15-23.

3. Worthington, M. H., "An Introduction to Geophysical Tomography," *First Break*, V. 2, No. 11, 1984, pp. 20-26.

4. Kak, A., and Slaney, M., *Principles of Computerized Tomographic Imaging*, IEEE Press, New York, 1988.

5. Jackson, M. J., and Tweeton, D. R., "3-Dtom: Three-Dimensional Geophysical Tomography," *Report of Investigations* 9617, U.S. Bureau of Mines, 1996.

6. Jackson, M. J.; Tweeton, D. R.; Scott, D. F.; and Williams T., "Three-Dimensional Imaging of Underground Mine Structures using Geophysical Tomography, with Tests for Resolution and Robustness," *Proceedings*, Third Canadian Conference on Computer Applications in the Mineral Industry, Quebec, 1995.

7. Hermann, L.; Dianiska, L.; and Verboci, J., "Curved Ray Algebraic Reconstruction Technique Applied in Mining Geophysics," *Geophysical Transactions*, Eotvos Lorand Geophysical Institute of Hungary, V. 28, No. 1, 1982, pp. 33-46.

8. Krajewski, C.; Dresen, L.; Gelbke, C.; and Ruter, H., "Iterative Tomographic Methods to Locate Seismic Low-Velocity Anomalies: A Model Study," *Geophysical Prospecting*, V. 37, 1989, pp. 717-751.

9. Singh, R. P., and Singh, Y. P., "RAYPT—A New Inversion Technique for Geotomographic Data," *Geophysics*, V. 56, No. 8, Aug. 1991, pp. 1215-1227.

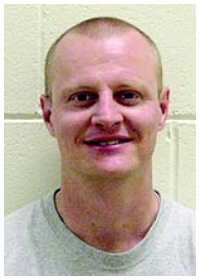

***Kevin L. Rens**, P.E., is an associate professor in the Department of Civil Engineering, University of Colorado at Denver. He received his BS in civil engineering from Iowa State University (ISU), Ames, Iowa, in 1988. From 1987 to 1994, he was employed at ISU, working on a research project titled Repair, Evaluation, Maintenance, and Rehabilitation (REMR) of navigation infrastructure for the U. S. Army Corps of Engineers. During that time, he earned advanced degrees in structural engineering. His research interests include infrastructure asset management, failure analysis and nondestructive testing of infrastructure, and concrete and cement materials science.*

***David J. Transue** is a consulting engineer and has been at Atkinson-Noland & Associates since 1998. He has published papers relating to the development of test methods for the evaluation of masonry and concrete structures, and on ultrasonic imaging techniques for concrete infrastructure. He received an MS in civil engineering from the University of Colorado at Denver. He specializes in nondestructive evaluation, preservation of historic masonry structures, and the durability of materials.*

because the data set consists of a limited number of ray paths. Instead, the cross-sectional area in which the rays travel is divided into a number of pixels, each of which has one value of slowness. The line integral over the ray path is then approximated by the summation

$$Travel\ Time = \sum_{j=1}^{m} s * dl$$

where: m = number of pixels in the ray path
s = slowness (inverse velocity) of pixel j
dl = distance traveled by ray in pixel j

The results of these travel-time calculations for each ray are then compared with the measured travel times of the rays. The value of velocity in each pixel is then adjusted so that the model more closely reflects the measured data. This process is repeated until the difference between the measured travel times and travel times calculated by tracing simulated rays through the model of the velocity field (the residual error) is sufficiently low. The values of the imaging parameter in each pixel are then associated with colors or contrasts to create an image. Several additional publications further detail straight-path tomomgraphy.[3, 4, 5]

Resolution, Uniqueness, and Curved-Ray Tomography

The resolution of acoustic tomographic images is limited by the thoroughness of ray-path coverage, the wavelength of the acoustic waves, and by refraction and diffraction of energy around low velocity regions.[6] Ray-path coverage and wavelength are functions of the data collection processes, while refraction and diffraction effects are dependent on the velocity gradations within the medium. Many algorithms have been developed to model curved ray paths due to refraction and diffraction.[4, 7, 8, 9]